

Numerical computation of discrete differential scattering cross sections for Monte Carlo charged particle transport

The Faculty of Oregon State University has made this article openly available.
Please share how this access benefits you. Your story matters.

Citation	Walsh, J. A., Palmer, T. S., & Urbatsch, T. J. (2015). Numerical computation of discrete differential scattering cross sections for Monte Carlo charged particle transport. <i>Nuclear Engineering and Design</i> , 295, 674-678. doi:10.1016/j.nucengdes.2015.07.018
DOI	10.1016/j.nucengdes.2015.07.018
Publisher	Elsevier
Version	Version of Record
Terms of Use	http://cdss.library.oregonstate.edu/sa-termsfuse



Numerical computation of discrete differential scattering cross sections for Monte Carlo charged particle transport



Jonathan A. Walsh^{a,*}, Todd S. Palmer^b, Todd J. Urbatsch^c

^a Department of Nuclear Science and Engineering, Massachusetts Institute of Technology, 77 Massachusetts Avenue, 24-107, Cambridge, MA 02139, United States

^b Department of Nuclear Engineering and Radiation Health Physics, Oregon State University, 116 Radiation Center, Corvallis, OR 97331, United States

^c XTD-IDA: Theoretical Design, Integrated Design and Assessment, Los Alamos National Laboratory, Los Alamos, NM 87545, United States

HIGHLIGHTS

- Generation of discrete differential scattering angle and energy loss cross sections.
- Gauss–Radau quadrature utilizing numerically computed cross section moments.
- Development of a charged particle transport capability in the Milagro IMC code.
- Integration of cross section generation and charged particle transport capabilities.

ARTICLE INFO

Article history:

Received 9 June 2015

Accepted 12 July 2015

Available online 4 August 2015

ABSTRACT

We investigate a method for numerically generating discrete scattering cross sections for use in charged particle transport simulations. We describe the cross section generation procedure and compare it to existing methods used to obtain discrete cross sections. The numerical approach presented here is generalized to allow greater flexibility in choosing a cross section model from which to derive discrete values. Cross section data computed with this method compare favorably with discrete data generated with an existing method. Additionally, a charged particle transport capability is demonstrated in the time-dependent Implicit Monte Carlo radiative transfer code, Milagro. We verify the implementation of charged particle transport in Milagro with analytic test problems and we compare calculated electron depth–dose profiles with another particle transport code that has a validated electron transport capability. Finally, we investigate the integration of the new discrete cross section generation method with the charged particle transport capability in Milagro.

© 2015 Elsevier B.V. All rights reserved.

1. Introduction

Differential charged particle scattering cross sections are highly peaked towards small scattering angles and small energy losses. Single-event Monte Carlo charged particle transport can be computationally demanding because of its explicit simulation of each of these interactions (Jenkins et al., 1988). Condensed history algorithms have been investigated as a means of alleviating this computational burden (Berger, 1963). These algorithms enforce a distance-to-collision that is greater than the physical distance-to-collision that would be observed in a single-event Monte Carlo simulation. Scattering angles and energy losses are then sampled at these artificial spatial step sizes. Because the

distance between collisions is increased, the number of simulated interactions and the simulation runtime are reduced. However, as a result of the fixed, artificial step sizes they employ, condensed history algorithms can have difficulties at material interfaces.

We look at a method for reducing the number of simulated interactions and runtime via alternative cross sections. Options for this sort of modified cross section data include discrete differential scattering angle and energy loss cross section values (Franke and Prinja, 2005) and cross section values obtained from simplified continuous models. Any method for improving the computational efficiency of a simulation should also preserve the essential physics of single-event methods so as to retain the accuracy of the transport solution. In order to maintain the accuracy of the results produced in simulations utilizing modified cross section data, the modified data should preserve higher order moments of the original cross section data (Lewis, 1950).

* Corresponding author. Tel.: +1 5035051872.
E-mail address: walshjon@mit.edu (J.A. Walsh).

2. Generation of discrete differential cross sections

Previous work by Franke and Prinja uses moment-preserving discrete scattering cross sections to speed up charged particle transport simulations relative to the single-event approach (Franke and Prinja, 2005). That work makes use of recursion relationships described by Morel (Morel, 1979) to generate modified moments of the weight function defined by the selected cross section model. These modified moments are then used as inputs for the algorithm developed by Sloan (1983), and extended in work by Morel et al. (1996), for generating discrete cross section values.

In the procedure presented here, the required modified moments of the cross section weight function are computed through numerical integration rather than recursion relationships. For this numerical integration, we use the QAG algorithm from the GNU Scientific Library (QAG adaptive integration, 2015). This algorithm is an adaptive integration scheme based on a 61-point Gauss–Kronrod rule. Numerical integration in the computation of the modified moments provides more flexibility in the selection of scattering cross section models and makes the use of more complex cross section models or discrete cross section data possible.

As in Sloan’s algorithm, once modified moments are computed, a Gauss–Radau quadrature is used to generate discrete scattering angle and energy loss cross section values. Taking advantage of a property of Gauss–Radau quadrature schemes, we are able to fix a node at a scattering angle of zero and also an energy loss of zero. Because differential charged particle scattering cross sections are highly forward peaked towards small scattering angles and energy losses, the discrete cross section values fixed at these points account for a substantial fraction of all interactions. The large zero-angle change and zero-energy loss cross sections can be subtracted from both sides of the transport equation, effectively increasing the mean-free-path between collisions and reducing simulation runtime. Retaining the other discrete cross section values from the quadrature preserves the higher order moments of the data in order to capture important physical information.

For this work, the Gaussian quadrature algorithm presented by Fernandes and Atchley (2006) is modified to perform a Gauss–Radau quadrature. This algorithm requires recursion coefficients for polynomials that are orthogonal with respect to some weight function. In the case of generating discrete cross section values, the continuous cross section model serves as the weight function. The required recursion coefficients are obtained from a modified Chebyshev algorithm described by Gautschi (1994). As inputs for the modified Chebyshev algorithm, the numerically computed modified moments of the weight function and coefficients for a set of unweighted orthogonal polynomials are required. The n th modified moment of the elastic scattering cross section, σ_{el} , is given by

$$\sigma_{el,n}(E) = \int_{-1}^1 \sigma_{el}(\vec{r}, \mu_0, E) p_n(\mu_0) d\mu_0 \quad (1)$$

for incident particle energy, E , and scattering angle cosine, μ_0 . The n th modified moment of the inelastic scattering cross section, σ_{in} , is given by

$$\sigma_{in,n}(E) = \int_0^{1-2Q_{min}/E} \sigma_{in}(E, \xi(E \rightarrow E')) p_n(\xi) d\xi \quad (2)$$

with the minimum energy loss, Q_{min} , taken to be the mean excitation energy of the material through which the particle is traveling, as suggested by Franke and Prinja (2005). The orthogonal polynomial coefficients come from the monic Legendre polynomials. This

set of polynomials is defined by a three term recursion relationship with the terms

$$\begin{aligned} p_{-1} &= 0; \\ p_0 &= 1; \end{aligned} \quad (3)$$

$$p_{k+1}(\lambda) = (\lambda - a_k)p_k(\lambda) - b_k p_{k-1}(\lambda)$$

where the polynomial coefficients are defined as

$$\begin{aligned} a_k &= 0; \\ b_k &= \frac{n^2}{4n^2 - 1}. \end{aligned} \quad (4)$$

In our initial studies, we have chosen to use the screened Rutherford cross section model to generate discrete elastic scattering cross sections. The screened Rutherford cross section is given by

$$\sigma_{el}(\vec{r}, \mu_0, E) = \sigma_{el,0} \frac{2\eta(1 + \eta)}{(1 + 2\eta - \mu_0)^2} \quad (5)$$

with the energy-dependent screening parameter, η . The continuous screened Rutherford elastic scattering cross section model can be made discrete by setting

$$\sigma_{el}(\vec{r}, \mu_0, E) = \sum_{i=1}^{M-1} w_i(E) \delta(\mu_0 - x_i(E)) + w_0(E) \delta(\mu_0 - 1) \quad (6)$$

with weights, w_i and w_0 , and nodes, x_i , of a Gauss–Radau quadrature set corresponding to discrete cross section values. From the continuous cross section model, we generate discrete cross section values using the process described above. The peaking of the screened Rutherford cross section towards zero-angle change can be seen in Fig. 1, which compares the continuous cross section model to the discrete cross section values obtained through both our method

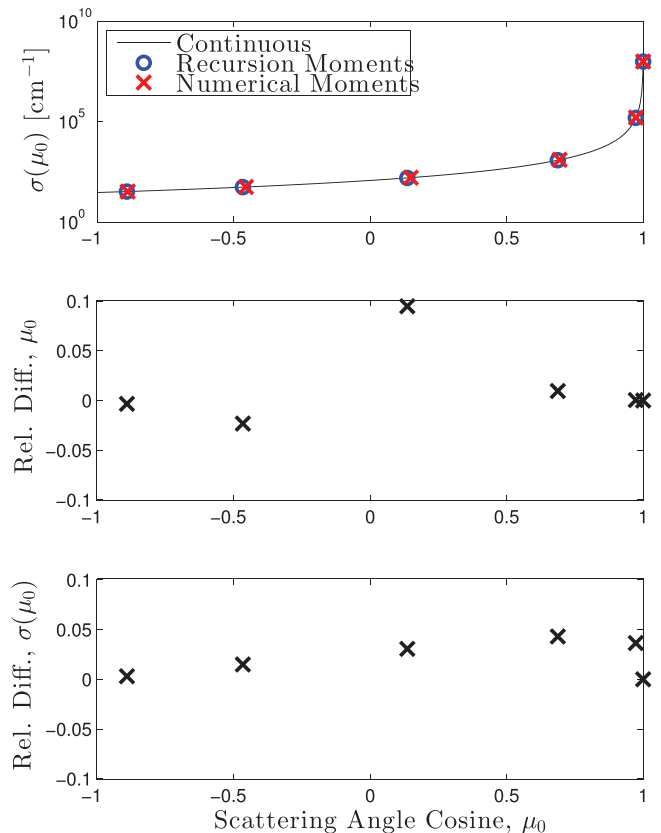


Fig. 1. Elastic scattering cross sections for 311 keV electrons with relative differences in discrete cross sections and scattering cosines.

and that of Franke and Prinja (2005). Relative differences between the two sets of discrete scattering cosines and differential cross sections are also shown.

In a similar fashion, the discrete inelastic scattering cross section values we generate for energy losses are obtained from a weight function described by the Rutherford cross section model,

$$\sigma_{\text{in}}(\vec{r}, E \rightarrow E') = \frac{Z\rho N_A 2\pi R_0^2 m_e c^2}{A\beta^2 Q^2}; \quad (7)$$

$$Q_{\text{min}} \leq Q \leq \frac{E}{2}$$

where

$$\beta^2 = \frac{\tau(\tau + 2)}{(\tau + 1)^2}; \quad (8)$$

$$\tau = \frac{E}{m_e c^2}.$$

Terms in the Rutherford cross section model include the atomic number of the material, Z ; density of the material, ρ ; Avogadro's number, N_A ; classical electron radius, R_0 ; electron rest mass energy, $m_e c^2$; atomic weight of the material, A ; and energy loss, Q . The continuous Rutherford inelastic scattering cross section model is made discrete with a Gauss–Radau quadrature by setting

$$\sigma_{\text{in}}(E \rightarrow E') = \sum_{i=1}^{M-1} w_i(E) \delta(Q - x_i(E)) + w_0(E) \delta(Q). \quad (9)$$

With a convenient change of variables that allows us to fix a discrete inelastic scattering cross section at an energy loss of zero, Eq. (9) can be recast as

$$\sigma_{\text{in}}(E, \xi(E \rightarrow E')) = \sum_{i=1}^{M-1} w'_i(E) \delta(\xi - x'_i(E)) + w'_0(E) \delta(\xi - 1); \quad (10)$$

$$\xi = 1 - \frac{2Q}{E}.$$

As with the screened Rutherford model, we generate discrete cross section values from the continuous Rutherford cross section model through the process previously described. The high peaking of the Rutherford cross section towards zero-energy loss interactions is shown in Fig. 2, which compares the continuous cross section model to the discrete cross section values obtained through both our method and that of Franke and Prinja (2005). Again, relative differences between the two sets of discrete nodes (i.e. energy losses) and differential cross sections are shown.

The two processes for computing modified moments of the cross section weight function produce sets of discrete values that differ from one another. The relative differences in discrete scattering angles and energy losses, and corresponding cross section values computed with our method, as compared to the values computed with the method described by Franke and Prinja (2005), are shown in Figs. 1 and 2. Relative differences in both the elastic and inelastic scattering cross section values at the selected energy, 311 keV, are typically a few percent, with all being less than 10%. However, depending on the application, the relative difference between individual discrete differential cross sections may be too extreme of a metric, because, as we show in Section 3.2, the differences in integral dose calculation results from the different methods are not as large as the differences in the discrete differential data.

3. Demonstration of charged particle transport in Milagro

In addition to investigating an alternate method for generating discrete scattering cross sections, we demonstrate a charged particle transport capability in the Milagro code package (Urbatsch and Evans, 2006). Milagro is a time-dependent Implicit Monte Carlo

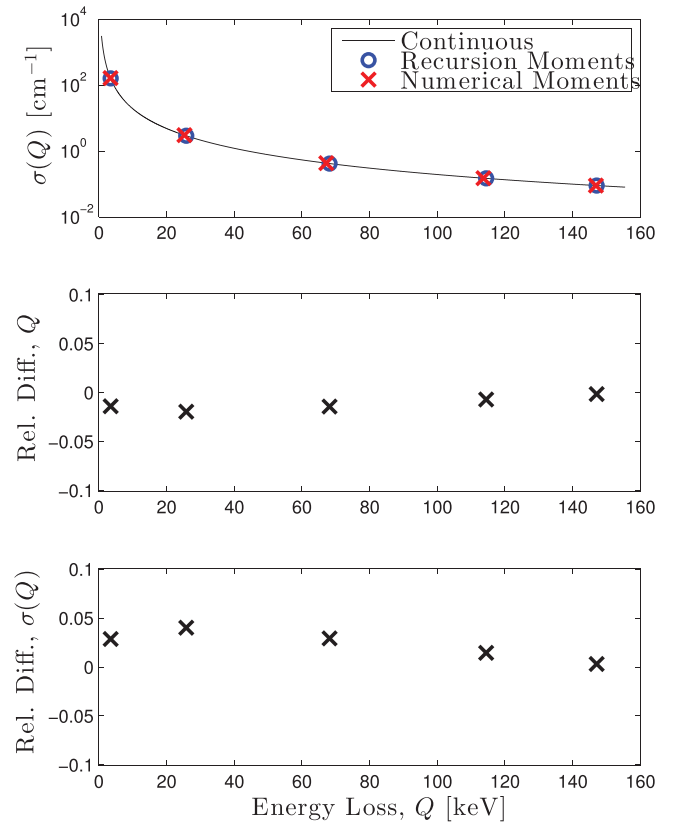


Fig. 2. Inelastic scattering cross sections for 311 keV electrons with relative differences in discrete cross sections and energy losses.

code developed at Los Alamos National Laboratory for thermal radiative transfer problems. Modifications to Milagro as part of the implementation of a charged particle transport capability include the ability to utilize the discrete cross section data generated in the first part of this work and disabling or altering physics routines so as to simulate charged particle transport rather than radiative transfer. The following sections are dedicated to the testing of Milagro's charged particle transport capability as well as the testing of the discrete cross section data generation method described in the previous section.

3.1. Testing of the implementation in Milagro

Two simple, common test problems with analytical solutions are used to verify the implementation of charged particle transport in Milagro. We describe these test problems briefly, but, due to their ubiquity, we do not present results. The first problem has particles normally incident on one face of a one-dimensional slab. The slab is composed of a material with an interaction cross section of zero and, as a result, particles stream through, unattenuated. The result of this problem agrees with the analytical solution exactly. The second problem again has particles normally incident on one face of a one-dimensional slab. In this case, the slab is a purely absorbing material with a constant interaction cross section. With an increasing number of particles, the result of this simulation converges to the expected exponential attenuation given by the analytical solution.

Next, we compare results from Milagro to results obtained by Franke and Prinja with a modified Integrated TIGER Series (ITS) code (Franke et al., 2005) for a time-independent electron dose test problem. The test problem consists of 250 keV electrons normally incident on a thin gold foil. One million particle histories are

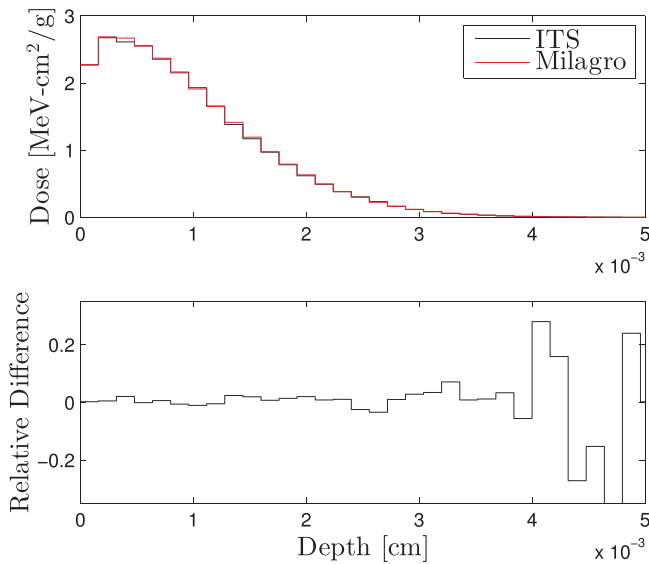


Fig. 3. Depth-dose profiles for testing of the Milagro implementation.

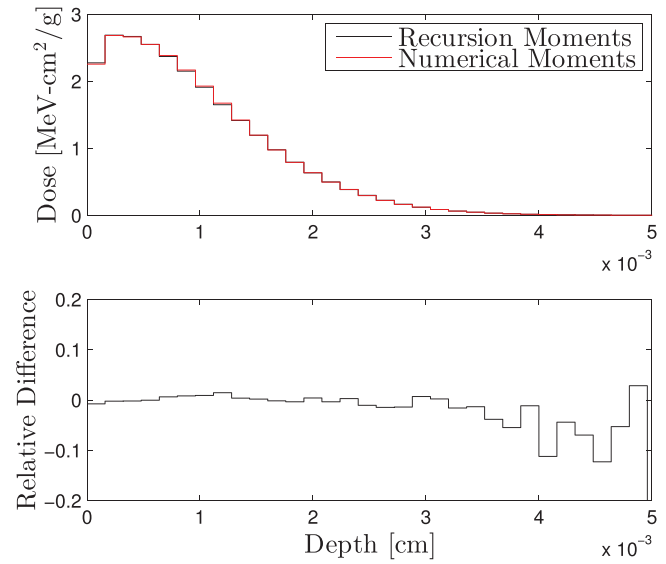


Fig. 4. Depth-dose profiles for testing of discrete cross section data.

simulated. Eighteen non-uniform energy groups, each consisting of five discrete cross section values, are generated and used in the calculation. A so-called nearest-neighbor energy group treatment is used in the Milagro implementation. This treatment consists of determining the midpoint energy of each energy group, identifying which midpoint energy an incident particle is closest to, and utilizing the cross section data for the energy group corresponding to the identified midpoint energy.

In order to isolate the implementation as the focus of this comparison, Milagro and ITS both use the discrete cross section data previously generated through Sloan’s algorithm. The depth-dose profiles calculated by each code are plotted in Fig. 3 along with the relative difference in the calculated profiles as a function of depth. Examining Fig. 3, the relative difference in calculated dose that is attributable to the implementation is less than a few percent at depths where the dose is non-negligible. At depths in the foil where the dose is negligible, statistical fluctuations dominate and the relative difference increases above a few percent.

3.2. Testing of discrete cross section data

With a satisfactory verification of the implementation of charged particle transport in Milagro, attention is turned to testing of the discrete cross section generation method through testing of the data produced with the method. Considering the same test problem, the data is tested by comparing dose results calculated using discrete cross sections generated using the new method with the results calculated using the discrete cross sections generated by Franke and Prinja. Dose results calculated with ITS using the recursion moment-based discrete cross sections obtained from Sloan’s algorithm have been shown to agree to within a few percent with single-event calculations up to depths at which dose becomes negligible (Franke and Prinja, 2005).

To isolate the effects of differences in the discrete cross section data on the dose calculation results, both simulations are performed in Milagro with the only difference being the data utilized by the code. The depth-dose profiles calculated with each set of data are plotted in Fig. 4 along with the relative difference in the profiles versus depth. As in the verification of the implementation, at depths where the dose is non-negligible, the relative difference in dose owing to differences in the cross section data is less than a few percent. Again, at depths where the dose becomes negligible, the

relative difference increases above a few percent due to statistical fluctuations.

3.3. Testing of discrete cross section data integrated with Milagro

In an effort to examine the integration of the discrete cross section generation method with the implementation of the charged particle transport capability in Milagro, we consider a second test problem. The second problem has 20 MeV electrons normally incident on a slab of water. One million particle histories are simulated. Again, eighteen non-uniform energy groups, each with five discrete cross section values, are generated and used in the calculation. The same nearest-neighbor energy group treatment is used.

The integration of the discrete cross section generation method with the implementation of the charged particle transport capability in Milagro is assessed through a comparison of the depth-dose profile for the second test problem calculated by Milagro using the generated discrete cross section data with the depth-dose profile calculated by ITS using discrete data obtained from moments computed with recursion relationships. The two depth-dose profiles

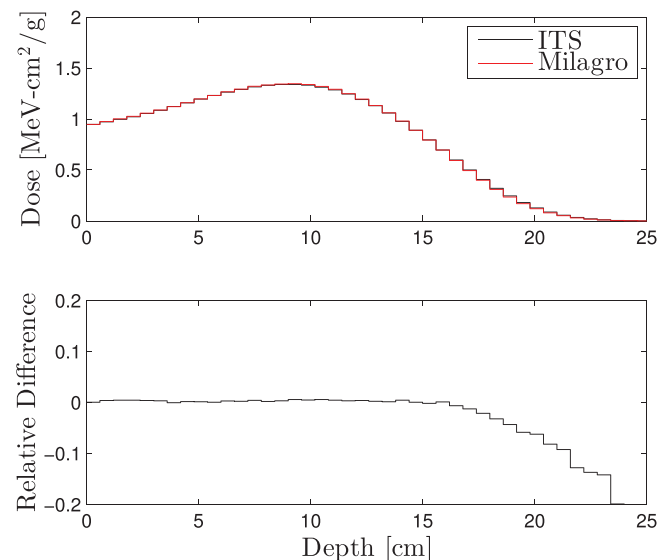


Fig. 5. Depth-dose profiles for combined testing of Milagro and generated data.

and their relative difference are plotted in Fig. 5. As with the individual testing of both the discrete data and the implementation in Milagro, the relative difference resulting from the integration of the two is less than a few percent at depths where dose is significant. However, at significant depths, where range straggling occurs and little energy is deposited, dominant statistical fluctuations in the relative difference are not present. Instead, Milagro consistently calculates a lower dose value than ITS. Past a certain depth, the magnitude of the relative difference increases with depth in a monotonic fashion, as can be seen in Fig. 5. For the same test problem, single-event simulations have also been shown to produce depth–dose profiles that are lower in magnitude, at significant depths, than profiles calculated by ITS (Franke and Prinja, 2005). As is the case with the Milagro results, the magnitude of the relative difference between single-event and ITS profiles increases monotonically with depth.

4. Conclusions

In this work we have presented a method for generating discrete differential charged particle scattering cross sections. The method's use of numerical integration rather than recursion relationships to generate moments of the data makes it more general than those previously investigated. Electron depth–dose profiles calculated with discrete cross section data generated with this method are shown to be in good agreement with depth–dose profiles calculated using discrete cross sections derived from recursion-based moments. Previously, these depth–dose profiles have been shown to agree with single-event simulations to within a few percent at depths where the dose is significant. In addition, a charged particle transport capability utilizing cross section data generated with this method is demonstrated in the Milagro code. Electron depth–dose profiles calculated with Milagro, using cross sections generated with the new method, are shown to agree with the depth–dose profiles calculated with the ITS code to within a few percent at depths where the dose is non-negligible. The profiles calculated with the ITS code have been previously shown to agree with single-event simulation results in the same manner.

5. Future work

The presented verification and comparisons of Milagro's charged particle transport capability rely solely on steady-state test problems. In order to confidently utilize Milagro for time-dependent charged particle transport simulations, verification against time-dependent test problems is necessary. Statistical analyses of the presented results would provide further verification of the cross section generation method and its integration with

Milagro. Assessment of convergence using batch statistics is one possible area for analysis. An investigation of the monotonically increasing relative difference magnitude observed in Fig. 5 is also of interest. There is room for improving Milagro's charged particle capability by accounting for the transport of secondary particles. The production of knock-on electrons is not considered here. Also, the application of adjoint-based variance reduction techniques, previously employed for Monte Carlo neutral particle transport (Coveyou et al., 1967), can be explored for charged particles. Finally, in addition to the electron scattering cross section models considered in this work, other cross section models, for both electron and heavy charged particle scattering, can be investigated.

Acknowledgments

The Computational Physics and Methods group, CCS-2, at Los Alamos National Laboratory is acknowledged for providing resources to make this work possible. The authors also thank Brian C. Franke of Sandia National Laboratories for his assistance in reviewing previous work in this area and allowing access to data with which to compare results.

References

- Berger, M., 1963. Monte Carlo calculation of the penetration and diffusion of fast charged particles. *Methods Comput. Phys.* 1, 135–215.
- Coveyou, R., Cain, V., Yost, K., 1967. Adjoint and importance in Monte Carlo application. *Nucl. Sci. Eng.* 27, 219–234.
- Fernandes, A., Atchley, W., 2006. Gaussian quadrature formulae for arbitrary positive measures. *Evol. Bioinform. Online* 2.
- Franke, B., Prinja, A., 2005. Monte Carlo electron dose calculations using discrete scattering angles and discrete energy losses. *Nucl. Sci. Eng.* 149 (1).
- Franke, B., Kensek, R., Laub, T., 2005. ITS version 5.0: The Integrated TIGER Series of coupled electron/photon Monte Carlo transport codes with CAD geometry. *Tech. Rep. SAND-2004-5172*. Sandia National Laboratories.
- Gautschi, W., 1994. Algorithm 726: ORTHPOL – a package of routines for generating orthogonal polynomials and Gauss-type quadrature rules. *ACM Trans. Math. Softw. (TOMS)* 20 (1).
- Jenkins, T.M., Nelson, W.R., Rindi, A. (Eds.), 1988. *Monte Carlo Transport of Electrons and Photons*. Plenum Press.
- Lewis, H., 1950. Multiple scattering in an infinite medium. *Phys. Rev.* 78, 526–529.
- Morel, J.E., Lorence, L.J., Kensek, R.P., Halbleib, J.A., Sloan, D.P., 1996. A hybrid multigroup/continuous-energy Monte Carlo method for solving the Boltzmann–Fokker–Planck equation. *Nucl. Sci. Eng.* 124 (3), 369–389.
- Morel, J., 1979. On the validity of the extended transport cross-section correction for low-energy electron transport. *Nucl. Sci. Eng.* 71, 64–71.
- QAG adaptive integration, https://www.gnu.org/software/gsl/manual/html_node/QAG-adaptive-integration.html (January 2015).
- Sloan, D., 1983. A new multigroup Monte Carlo scattering algorithm suitable for neutral and charged-particle Boltzmann and Fokker–Planck calculations, *Tech. Rep. SAND-83-7094*. Sandia National Laboratories.
- Urbatsch, T., Evans, T., 2006. Milagro version 2 – an implicit Monte Carlo code for thermal radiative transfer: capabilities, development, and usage, *Tech. Rep. LA-14195-MS*. Los Alamos National Laboratory.